MATEMATIKA, 2012, Volume 28, Number 2, 109–125

Unsteady Mixed Convection Flow over a Cylinder of Elliptic Cross Section near Forward Stagnation Point

[1]Madina Jamaludin, [2]Nurul Farahain Mohammad, [3]Sharidan Shafie and [4]Anati Ali

[1] Faculty of Computers and Mathematical Sciences,
Universiti Teknologi MARA, 85000 Segamat, Johor, Malaysia.

[2] Department of Computational and Theoretical Sciences, Kulliyyah of Science,
International Islamic University Malaysia, 25200 Kuantan, Pahang, Malaysia.

[2,3,4]Department of Mathematical Sciences, Faculty of Science,
Universiti Teknologi Malaysia, 81310 Skudai, Johor, Malaysia.

e-mail: [1]madinajamaludin@gmail.com, [2]nurul.farahain.mohammad@gmail.com
[3]sharidan@utm.my, [4]anati@utm.my

Abstract The unsteady mixed convection flow over a cylinder of elliptic cross section when the major axis is horizontal (blunt orientation) or vertical (slender orientation) near forward stagnation point is studied. The unsteadiness is due to an impulsive motion on the free stream. The governing boundary layer equations are first reduced into a non-dimensional form, and then transformed into a set of non-similar boundary layer equations, which are solved numerically using an efficient implicit finite-difference method known as Keller-Box method. The numerical results are obtained for various values of the Prandtl number, Pr, the mixed convection parameter, α and parameter for blunt and slender orientation, ω. The effects of these parameters on velocity profiles, temperature profiles as well as Nusselt number are presented through graphs and tables. The results show that as the mixed convection parameter, α is increased, the velocity of the fluid is increased but the temperature of the fluid is decreased, for both blunt and slender orientations. Furthermore, the slender orientation gives earlier separation times for opposing flow while there is no separation of flow detected for the assisting flow.

Keywords unsteady flow; mixed convection; cylinder of elliptic cross section; forward stagnation point.

2010 Mathematics Subject Classification 76B99; 76R99

1 Introduction

In these recent years, unsteady flows have become significant in both different category of fluid mechanics and convection in heat and mass transfer. The problem of unsteady convective heat transfer has long been a major subject in the heat transfer theory because of its great importance from both theoretical and practical viewpoint. The extra independent variable time which has been considered in the unsteady problem can increase the complexity of its solving procedure. The unsteady effects can arise in two situations. The first situation is due to self-induced motion of the body and the second situation is due to the fluctuations or nonuniformities in the surrounding fluid. Besides that, some devices are required to execute time-dependent motion in order to perform their basis functions [1].

In general, unsteady viscous phenomena play an important role in the reentry of space vehicles. Unsteady viscous flows have been studied quite widely and all the characteristic features of unsteady effects are now more or less familiar to fluids mechanists. The problem of unsteady mixed convection boundary layer flow of Newtonian and Non-Newtonian fluid

past a circular cylinder have been considered by Ingham and Merkin [2] and Ali *et al.* [3], respectively. In addition, the study of stagnation point flow has attract much attention because of its capability in providing the governing equations to be much simplified besides allowing the process of bringing out all the essential features. The stagnation point solution, though it may valid in a small region in the vicinity of stagnation point, may function as a starting solution for the solution over the entire body, as proven by Lok [4].

Many researchers had been working on elliptical cylinder problem. In 1977, Merkin [5] was working on steady free convection with elliptic cross section problem. A study on steady forced convection was conducted by D'Alessio *et al.* [6]. In 1995, Chadna [7] had been researching on flow past an elliptic cylinder. Choi and Lee [8] investigated turbulent boundary layer on elliptical cylinder. Khan *et al.* [9] solved the elliptical cylinder problem by using analytical approach. In this paper, the problem is solved using semi-analytical approach. Several type of flows had been considered previously such as laminar flow [5], [6], creeping flow [10], potential flow [11] and flow inclined to the stream [12]. Furthermore, various types of fluids were considered by researchers. Bhattacharyya and Pop [13], and Cheng [14] were working on elliptical cylinder problem with micropolar fluids. Cheng [15] were also investigating in porous media. There are studies conducted to investigate elliptical cylinder problem on power-law fluids by Bharti *et al.* [16], and Rao *et al.* [17].

On the other hand, different effects had been studied in understanding the behaviour of fluid flows. Facas [18] had considered elliptical cylinder surface as a heat source. The effect of thermal radiation was investigated by Hossain *et al.* [19]. Cheng had been working on the effect of temperature dependent viscosity [14] and internal heat generation of an elliptical cylinder [20]. Ahmad *et al.* [21] had studied the constant surface heat flux of an elliptical cross section. Investigations on the effect of Grashof numbers, both small and large, were conducted by D'Alessio *et al.* [22], [23].But very few researches had considered the unsteadiness of the flow past an elliptic cylinder. The unsteady problem had been conducted on free convection [23] and forced convection [24] but so far, no research had considered the mixed convection. This study focuses on the unsteady mixed convection on the fluid flow past an elliptic cylinder.

2 Mathematical Formulation

Consider the problem of unsteady mixed convection flow over horizontal cylinders of elliptic cross section for both cases, blunt and slender orientations, near forward stagnation point subjected to constant surface temperature. This cylinder is placed in viscous and incompressible fluid of free stream velocity, U_∞ and ambient temperature, T_∞. The physical model of this problem is shown in Figure 1 while Figure 2 shows the physical model and coordinate system when the fluid is passing near forward stagnation point.

Following Merkin [5], we assume that at the same time, a uniform stream $0.5U_\infty$ at large distance from the cylinder is impulsively started and flows vertically upward. The dimensional governing equations for the problem considered in this study are as follows:

$$\frac{\partial \overline{u}}{\partial \overline{x}} + \frac{\partial \overline{v}}{\partial \overline{y}} = 0, \tag{1}$$

$$\frac{\partial \overline{u}}{\partial \overline{t}} + \overline{u}\frac{\partial \overline{u}}{\partial \overline{x}} + \overline{v}\frac{\partial \overline{u}}{\partial \overline{y}} = -\frac{1}{\rho}\frac{\partial \overline{p}}{\partial \overline{x}} + \frac{\mu}{\rho}\Big(\frac{\partial^2 \overline{u}}{\partial \overline{x}^2} + \frac{\partial^2 \overline{v}}{\partial \overline{y}^2}\Big) + \beta g\Big(\overline{T} - T_\infty\Big)\sin\Big(\phi\Big), \tag{2}$$

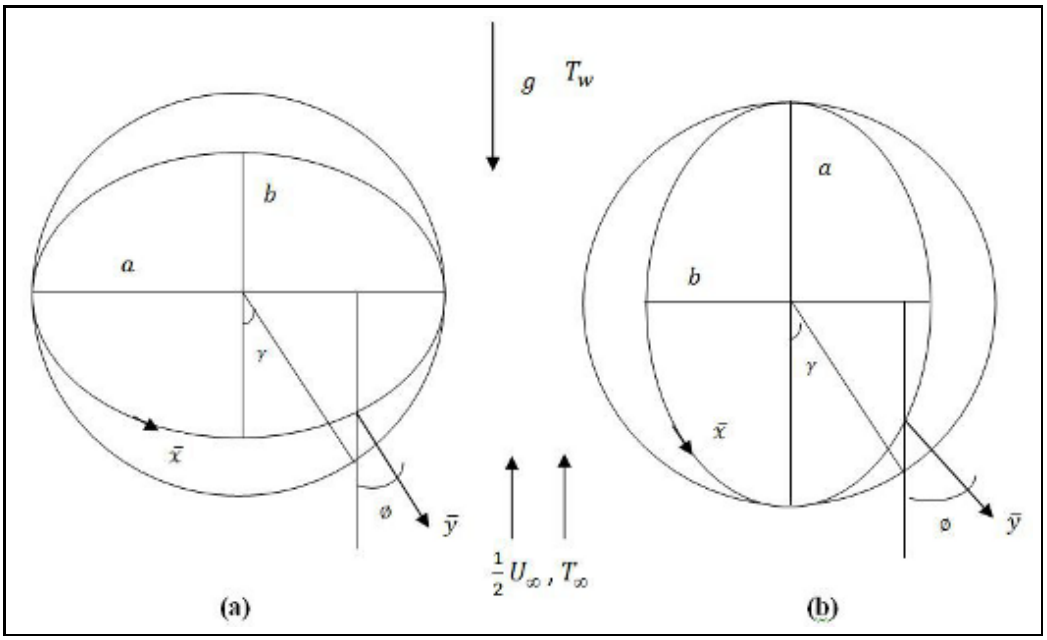

Figure 1: Physical model and coordinate system: (a) blunt orientation (b) slender orientation

$$\frac{\partial \overline{v}}{\partial \overline{t}} + \overline{u}\frac{\partial \overline{v}}{\partial \overline{x}} + \overline{v}\frac{\partial \overline{v}}{\partial \overline{y}} = -\frac{1}{\rho}\frac{\partial \overline{p}}{\partial \overline{y}} + \frac{\mu}{\rho}\Big(\frac{\partial^2 \overline{u}}{\partial \overline{x}^2} + \frac{\partial^2 \overline{v}}{\partial \overline{y}^2}\Big) - \beta g\Big(\overline{T} - T_\infty\Big)\cos\Big(\phi\Big), \tag{3}$$

$$\frac{\partial \overline{T}}{\partial \overline{t}} + \overline{u}\frac{\partial \overline{T}}{\partial \overline{x}} + \overline{v}\frac{\partial \overline{T}}{\partial \overline{y}} = \frac{c}{\rho C_p}\Big(\frac{\partial^2 \overline{T}}{\partial \overline{x}^2} + \frac{\partial^2 \overline{T}}{\partial \overline{y}^2}\Big), \tag{4}$$

subject to the following initial and boundary conditions

$$\begin{aligned} &\overline{t} < 0 : \overline{u} = \overline{v} = 0, \overline{T} = T_\infty \text{ for any } \overline{x}, \overline{y}, \\ &\overline{t} \geq 0 : \overline{u} = \overline{v} = 0, \overline{T} = T_w \text{ at } \overline{y} = 0 \text{ and } \overline{u} \to 0, \overline{T} \to T_\infty \text{ as } \overline{y} \to \infty. \end{aligned} \tag{5}$$

where ρ is the density of the fluid that flow pass, g is gravitational acceleration, β is the thermal expansion coefficient, $\frac{c}{\rho C_p}$ is the constant thermal diffusivity of the fluid and μ is the dynamic viscosity. Following Ali *et al.* [3], non-dimensional variables are introduced to obtain (1)-(4) in non-dimensional form as below:

$$\begin{aligned} x = \frac{\overline{x}}{a},\ y = \frac{\mathrm{Re}^{\frac{1}{2}}}{a}\overline{y},\ v = \mathrm{Re}^{\frac{1}{2}}\Big(\frac{\overline{v}}{U_\infty}\Big), \\ u = \frac{\overline{u}}{U_\infty},\ t = \frac{U_\infty}{a}\overline{t},\ T = \frac{(\overline{T} - T_\infty)}{(T_w - T_\infty)},\ p = \frac{1}{\rho}\frac{\overline{p}}{{U_\infty}^2} \end{aligned} \tag{6}$$

where Re= $\frac{aU_\infty}{v}$ is Reynolds number.

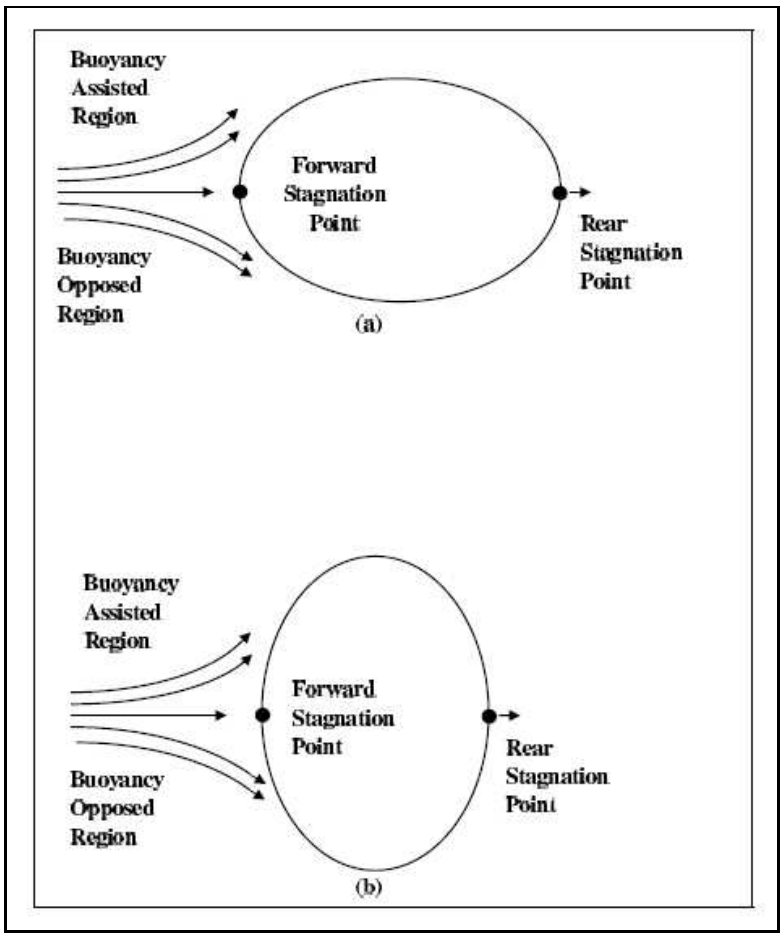

Figure 2: Physical model and coordinate system when the fluid is passing near stagnation point in (a)blunt orientation and (b)slender orientation.

Substituting these non-dimensional variables into (1)-(4), we obtain

$$\frac{\partial u}{\partial x}+\frac{\partial v}{\partial y}=0, \tag{7}$$

$$\frac{\partial u}{\partial t}+u\frac{\partial u}{\partial x}+v\frac{\partial u}{\partial y}=u_e\frac{du_e}{dx}+\frac{\partial^2 u}{\partial y^2}+\alpha T\sin\Big(\phi\Big), \tag{8}$$

$$\frac{\partial p}{\partial y}=0, \tag{9}$$

$$\frac{\partial T}{\partial t}+u\frac{\partial T}{\partial x}+v\frac{\partial T}{\partial y}=\frac{1}{\mathrm{Pr}}\Big(\frac{\partial^2 T}{\partial y^2}\Big). \tag{10}$$

where α is the mixed convection parameter which is denoted as $\alpha=\frac{\mathrm{Gr}}{\mathrm{Re}}$ and by applying Bernoulli equation, the pressure gradient may be expressed in free stream velocity, u_e, where $\frac{{u_e}^2}{2}+p=$ constant. Equation (9) shows that pressure is independent of y. Thus $\frac{dp}{dx}=-u_e\frac{du_e}{dx}$ and since the characteristic of equation (9) has been embedded in equation (8), the number of governing equations are then reduced into 3 equations.

According to Ali *et al.* [3], the flow near cooled body ($T_\infty < T_w$) leads to negative value of the mixed convection parameter, α ($\alpha<0$) since the buoyancy force would oppose the flow. This flow is called opposing flow. In contrast for assisting flow, when $T_\infty > T_w$ (heated body), the value of mixed convection parameter α leads to positive ($\alpha>0$) since buoyancy forces facilitate the convection motion. The initial and boundary conditions (5) become:

$$\begin{aligned}&t<0: u=v=T=0, \text{ for any } x,y,\\ &t\geq 0: u=v=0, T=1 \text{ at } y=0,\\ &u=u_e(x), T=0 \text{ as } y\to\infty.\end{aligned} \tag{11}$$

Then, similarity transformation with similarity variables as stated below is used to solve (7)-(10),

$$\psi=t^{\frac{1}{2}}u_e(x)f(x,\eta,t), \qquad T=s(x,\eta,t), \qquad \eta=\frac{y}{t^{1/2}}. \tag{12}$$

where ψ is the stream function defined as $u=\frac{\partial\psi}{\partial y}$ and $v=-\frac{\partial\psi}{\partial x}$.

Substituting (12) into (7)-(10), the following system of equations is obtained

$$\frac{\partial^3 f}{\partial\eta^3}+\frac{\partial\eta}{2}\frac{\partial^2 f}{\partial\eta^2}+t\frac{\partial u_e}{\partial x}\Big(1-\Big(\frac{\partial f}{\partial\eta}\Big)^2+f\frac{\partial^2 f}{\partial\eta^2}\Big)=t\frac{\partial^2 f}{\partial\eta\partial t}+tu_e\Big(\frac{\partial f}{\partial\eta}\frac{\partial^2 f}{\partial\eta\partial x}-\frac{\partial f}{\partial x}\frac{\partial^2 f}{\partial\eta^2}\Big)-t\alpha s\frac{\sin(\phi)}{u_e} \tag{13}$$

$$\frac{\partial^2 s}{\partial\eta^2}+\frac{\mathrm{Pr}\eta}{2}\frac{\partial s}{\partial\eta}+\mathrm{Pr}t\frac{\partial u_e}{\partial x}f\frac{\partial s}{\partial\eta}=\mathrm{Pr}t\Big(\frac{\partial s}{\partial t}+u_e\Big(\frac{\partial f}{\partial\eta}\frac{\partial s}{\partial x}-\frac{\partial f}{\partial x}\frac{\partial s}{\partial\eta}\Big)\Big) \tag{14}$$

subject to the initial and boundary conditions

$$\begin{aligned} &t<0: f=\frac{\partial f}{\partial \eta}=0, s=0, \text{for any } x, \eta, \\ &t\geq 0: f=\frac{\partial f}{\partial \eta}=0, s=1, \text{for any } \eta=0, \\ &\frac{\partial f}{\partial \eta}=1, s=0, \text{for any } \eta\to\infty, \end{aligned} \tag{15}$$

According to Ahmad *et al.* [21], there are two orientations to be considered in elliptic cross section; blunt orientation when the major axis is horizontal and when the major axis is vertical (slender orientation). x and $\sin(\phi)$ are given parametrically in terms of the eccentric angle γ by the following relations

$$x=\int_0^{\gamma}(1-e^2\sin^2 z)^{1/2}dz, \qquad \sin\phi=\frac{b}{a}\frac{\sin\gamma}{(1-e^2\sin^2\gamma)^{1/2}} \tag{16}$$

for the blunt orientation and

$$x=\int_0^{\gamma}(1-e^2\cos^2 z)^{1/2}dz, \qquad \sin\phi=\frac{b}{a}\frac{\sin\gamma}{(1-e^2\cos^2\gamma)^{1/2}} \tag{17}$$

for the slender orientation. b is the length of the semi-minor axis and e is the eccentricity given by $e=1-b/a^2$. Thus, $\omega=b/a$ or $\omega=(a/b)^2$ for blunt and slender orientations, respectively.

3 Solutions at Forward Stagnation Point

In this paper, only the case of forward stagnation point of a cylinder cross section is under consideration. Therefore, $\frac{\sin(\phi)}{u_e(x)}\to\omega$ as x tends to 0 according to Bhattacharyya *et al.* [13]. In addition, following Ingham and Merkin [2], it is assumed that $u_e(x)=\sin x$. Hence, $u_e=0$ and $\frac{\partial u_e}{\partial x}=1$ for the case of forward stagnation point. Thus, the governing equations become as follow at the forward stagnation point:

$$\frac{\partial^3 f}{\partial\eta^3}+\frac{\partial\eta}{2}\frac{\partial^2 f}{\partial\eta^2}+t\Big(1-\Big(\frac{\partial f}{\partial\eta}\Big)^2+f\frac{\partial^2 f}{\partial\eta^2}\Big)=t\frac{\partial^2 f}{\partial\eta\partial t}+t\alpha s\omega \tag{18}$$

$$\frac{\partial^2 s}{\partial\eta^2}+\frac{\mathrm{Pr}\eta}{2}\frac{\partial s}{\partial\eta}+\mathrm{Pr}tf\frac{\partial s}{\partial\eta}=\mathrm{Pr}t\Big(\frac{\partial s}{\partial t}\Big) \tag{19}$$

subject to the boundary conditions

$$\begin{aligned} &t\geq 0: f=\frac{\partial f}{\partial \eta}=0, s=1, \text{for } \eta=0, \\ &\frac{\partial f}{\partial \eta}=1, s=0, \text{for any } \eta\to\infty. \end{aligned} \tag{20}$$

4 Results and Discussions

The system of governing equations at forward stagnation point (17)-(18) is solved numerically by using the Keller-Box method which is the method that had been used by Ali *et al.* [3]. The numerical results obtained including velocity profile, temperature profile, the skin friction coefficient, the Nusselt number and the separation times near the forward stagnation point for blunt and slender orientations.

It is worth mentioning that when $\omega = 1$, the major axis and the minor axis are having the same length which means the object is now a circular cylinder. Therefore, in order to verify the present result, the value of separation time of the boundary layer near forward stagnation point ($x = 0$) for particular Prandtl number,Pr and mixed convection parameter,α are compared with those reported by Ali [25] for the case $k = 0$ (viscous fluid), as shown in Table 1. These results are found to be in excellent agreement. In Figure 3, the results obtained in this study had been compared with the results reported by Ingham and Merkin [2] and again, there are good agreement between the results. The mixed convection parameter,α considered in Figure 3 are in the range from -5 to 2.

Table 2 presents separation times along the cylinder of the elliptic cross section for some values of ω near forward ($x = 0$) stagnation point for Pr = 1 and $\alpha = -3$ (opposing flow) for both cases, blunt and slender orientations. It is noticed that the separation times are increased with increasing ω for the case of slender orientation. It is observed that the flow does not separate at the forward stagnation point when $\omega = 0.1$, 0.25 and 0.5 for the case of blunt orientation. The same behavior of the flow are observed when Pr = 7 and $\alpha = -3$. For this case, the separation times along the cylinder of the elliptic cross section near forward stagnation point for some values of ω are presented in Table 3. It can be seen that the separation times are increasing as the value of Pr increases for each value of ω on both cases, slender and blunt orientations at forward stagnation point. Table 4 shows the separation times along the cylinder of elliptic cross section near forward stagnation point ($x = 0$) when Pr = 7 and $\alpha = 1.25$ (assisting flow). The opposite trend can be seen where the separation times decrease with the increasing ω. When the case of slender orientation is considered, there are no separation times at forward stagnation point.

Figure 4 shows the variation of the separation times t_s for the boundary layer flow near the forward stagnation point ($x = 0$) of elliptic cylinder. In this figure, the mixed convection parameter α is considered in the range $-5 \leq \alpha \leq 2$ while the values of axis ratio b/a are taken as $b/a = 0.1, 0.25, 0.5, 0.75$ while $\omega = 100, 16, 4, 1.7778$ for slender orientation. It can be seen that near the forward stagnation point, the separation times for the case of blunt orientation are delayed compared to the case of slender orientation for the opposing flow ($\alpha < 0$). It is noted that there are no separation times obtained for assisting flow ($\alpha > 0$) and also when $\omega = 0.1, 0.25$. Furthermore, the separation times near forward stagnation point for the blunt orientation are higher than the separation times for slender orientation.

Figure 5 show the velocity profiles for some values of time t and mixed convection parameter α when Pr=1 for both cases, blunt and slender orientation, respectively. For the case of blunt orientation, it is clear that an increasing value of α leads to the increasing values of velocity profiles. Moreover, when $\alpha = 2$ (assisting flow), values of velocity are higher compared to the case of $\alpha = -3$ (opposing flow). Near the forward stagnation pooint, the values of velocity increase rapidly as the values of time, t increase when α is fixed. Furthermore, it is observed that as t increases, the boundary layer thickness

increases significantly. The similar behaviour of velocity profiles as discussed above are also observed for the case of slender orientation. Evidently, the values of velocity are increased by increasing α. In addition, when $\alpha = 2$ (assisting flow), the values of velocity are higher compared to the case when $\alpha = -3$ (opposing flow). It can be seen also for $\alpha = 2$ (assisting flow), the values of velocity are increased with increasing time t. However, a different behaviour is observed for $\alpha = -3$ (opposing flow) where as t increases, the value of velocity decreases. Moreover, it can be seen that the flow reversal occurred when $\alpha = -3$ (opposing flow) due to the fact that there are negative values of velocities. In addition, this region of flow reversal grows larger as t increases. Similarly to blunt orientation, as t increases,the boundary layer thickness increases sequencely.

Figure 6 display the velocity profiles near the forward stagnation point of the elliptic cylinder for various values of ω when Pr=1 and Pr=7 for the case of slender orientation and blunt orientation, respectively. It is noticed that the values of velocity decreases with increasing ω for both cases. As expected, flow reversal occurred for the case of slender orientation as shown in Figure 6(b) due to the fact that there are velocities with negative values. These regions of flow reversal grow larger when the value of ω becomes greater. It can be seen from these figures, the region of flow reversal are larger when Pr=1 compared to the case of Pr=7.

Figure 7 portray the velocity profiles near the forward stagnation point of the elliptic cylinder for various values of Pr for the case of slender orientation ($\omega = 4$) and blunt orientation ($\omega = 0.5$) when $t = 0.15$ and $\alpha = 1$. It is observed that the value of velocity decreases as the Prandtl number, Pr increases.

Figure 8 demonstrate the temperature profiles for some value of time ,t and mixed convection parameter,α when Pr=1 for the case of blunt and slender orientations, respectively. For the case of blunt orientation, velocity decreases with increasing time,t. However,for the case of slender orientation, the temperature increases for $\alpha = -3$ (opposing flow) and decreases for $\alpha = 2$ (assisting flow) with increasing time t. For both cases, it is noted that, as t increases, the thickness of the thermal boundary layer decreased. A similar pattern can be observed when the value of α increases.

Figure 9 illustrate the temperature profiles for some values of ω and Pr when $t = 0.15$ and mixed convection parameter, $\alpha = -3$ for the case of blunt and slender orientations, respectively. It is noted that when the Prandtl number,Pr is fixed, the value of temperature unchanged with increasing ω for the case of blunt orientation. Nevertheless, different pattern can be seen for the case of slender orientation as shown in Figure 9(b). In this figure, it is observed that near the forward stagnation point the values of temperature increase with increasing ω for both Pr=1 and Pr=7. On the other hand, both cases show that the values of temperature decrease with increasing Prandtl number, Pr. In addition, the thermal boundary layer thickness also decreases significantly. According to Ahmad [21], it is due to the fact that an increasing Pr will lead to a decrease of thermal diffusivity where it leads to the decrement on energy transfer and thus, decreases the thermal boundary layer. These patterns of temperature profiles are similar to those produced by Ali [25] for the problem of unsteady forced convection of boundary layer from a circular cylinder in a micropolar fluid.

On the other hand, Figure 10 present the variation of the Nusselt number, $Nu\mathrm{Re}^{-1/2}$ versus t for various value of ω and Pr when $\alpha = -3$ for blunt and slender orientations. It can be seen that Nusselt number is unchanged with increasing ω for blunt orientation. In spite of this, different pattern is found for the case of slender orientation where the Nusselt

number decreases with increasing ω. In addition, it is observed that the Nusselt number is higher for the case of Pr=7 compared to the case of Pr=1. This pattern of Nusselt number is similar to those obtained by Ali [25] for the problem of unsteady mixed convection boundary layer from a circular cylinder in micropolar fluid.

The variation of the Nusselt number with t for various value of Pr near the forward stagnation point for both cases, blunt and slender orientations, respectively is shown in Figure 11. It is noticed that by increasing the value of Prandtl number, Pr will lead to an increase of Nusselt number.

Figure 12 display the variation of the Nusselt number with t for some values of ω and α near the forward stagnation point for blunt orientation and slender respectively. From this figure, it is noted that there are no effects of mixed convection parameter, α on the values of Nusselt number for blunt orientation. However, when slender orientation is considered, the Nusselt number is lower for the case of $\alpha = -3$ (opposing flow) compared to the case of $\alpha = 2$ (assisting flow) near the forward stagnation point. On the other hand, the skin friction $C_f \mathrm{Re}^{1/2}$ is given as $C_f \mathrm{Re}^{1/2} = \frac{u_e}{t^{1/2}} \left(\frac{\partial^2 f}{\partial \eta^2} \right)_{\eta=0}$. It is noticed that for the problem near the forward stagnation point, the values of skin friction, $C_f \mathrm{Re}^{1/2}$ are equal to zero since at this point the value of $u_e(x)$ is zero.

5 Conclusion

From the study conducted, it can be concluded that skin friction coefficient are equal to zero near the forward stagnation point. Near the forward stagnation point, it is found that the Nusselt number is fixed with increasing ω for the case of blunt orientation. However, for the case of slender orientation, the Nusselt number near the forward stagnation point is decreased. Furthermore, The velocity profiles for both blunt and slender orientations near the forward stagnation point are found to be increased due to the effect of increasing mixed convection parameter. In addition, as the mixed convection parameter increases, the temperature near the forward stagnation point is decreased for both cases, slender and blunt orientations. Also, near the forward stagnation point it is found that as the mixed convection parameter increases, the Nusselt number is fixed for the case of blunt orientation. However, for the case of slender orientation, the Nusselt number near the forward stagnation point is increased. Moreover, the increasing value of Prandtl number, Pr leads to a decrease in the velocity and temperature of the fluid for slender and blunt orientations near the forward stagnation point. Meanwhile, the Nusselt number is found to be increased due to the increasing of Prandtl number, Pr. For separation of flow near the forward stagnation point, the slender orientation gives the earlier separation times for opposing flow. Nevertheless, no separation times is detected for the assisting flow.

Acknowledgements

The authors would like to acknowledge the Research Management Centre UTM for the financial supports through vote numbers 4F019 and 03J62, and also a special thanks to International Islamic University Malaysia for the sponsorship under the Academic Trainee scheme.

Table 1: Comparison of separation time at forward stagnation point for Pr = 1 and $\alpha = -3$ when $\omega = 1$

stagnation point,x	Prandtl number,Pr	mixed convection parameter,α	Ali [25] separation time,t_s	Present separation time,t_s
0	1	-3	0.7012	0.7012

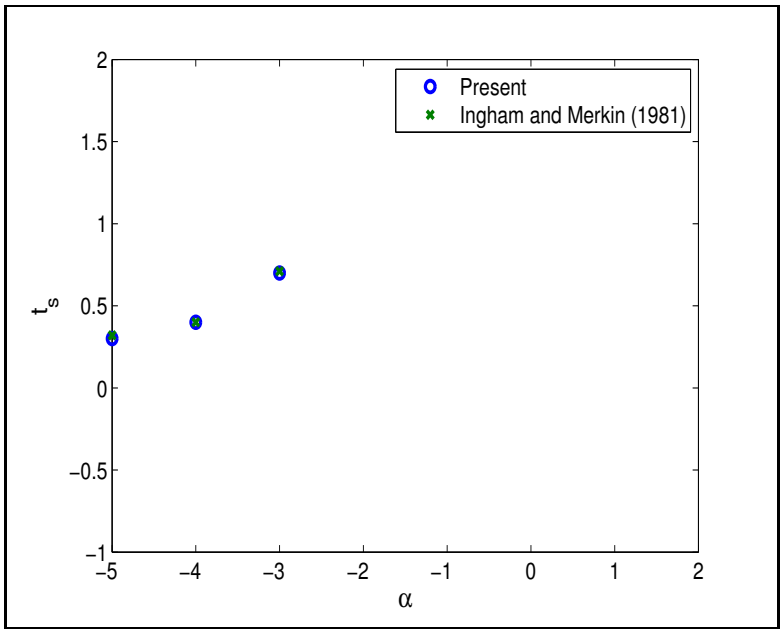

Figure 3: Variation of separation times near forward stagnation point when Pr=1

Table 2: The separation times, t_s of the cylinder of elliptic cross section near forward stagnation point ($x = 0$) for Pr=1 and $\alpha = -3$ (opposing flow)

ω	Blunt orientation,$\omega = \frac{b}{a}$				Slender orientation,$\omega = (\frac{a}{b})^2$			
	0.1	0.25	0.5	0.75	100	16	4	1.7778
t_s	-	-	-	1.5210	0.0033	0.0215	0.0954	0.2652

Table 3: The separation times, t_s of the cylinder of elliptic cross section near forward stagnation point ($x = 0$) for Pr=7 and $\alpha = -3$ (opposing flow)

ω	Blunt orientation,$\omega = \frac{b}{a}$				Slender orientation,$\omega = (\frac{a}{b})^2$			
	0.1	0.25	0.5	0.75	100	16	4	1.7778
t_s	-	-	-	-	0.0060	0.0361	0.1233	0.2252

Table 4: The separation times, t_s of the cylinder of elliptic cross section near forward stagnation point ($x = 0$) for Pr=7 and $\alpha = 1.25$ (assisting flow)

ω	Blunt orientation,$\omega = \frac{b}{a}$				Slender orientation,$\omega = (\frac{a}{b})^2$			
	0.1	0.25	0.5	0.75	100	16	4	1.7778
t_s	-	-	-	-	-	-	-	-

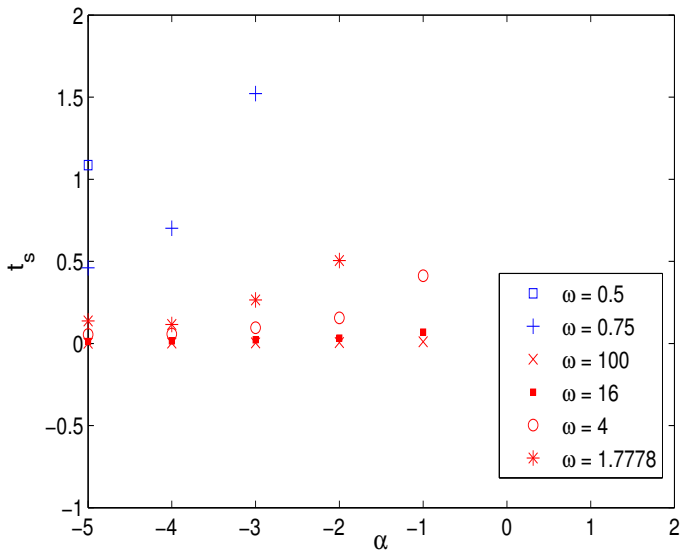

Figure 4: Variation of separation times near forward stagnation point when Pr=1 for various value of ω and α

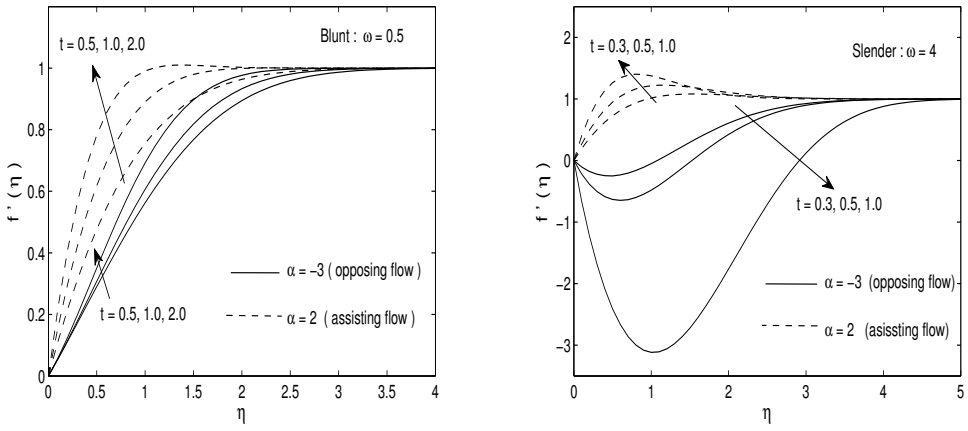

(a) (b)

Figure 5: The velocity profiles at $x = 0$ (forward stagnation point) for some values of α and t when Pr=1 in (a)blunt orientation ($\omega = 0.5$) and (b)slender orientation ($\omega = 4$)

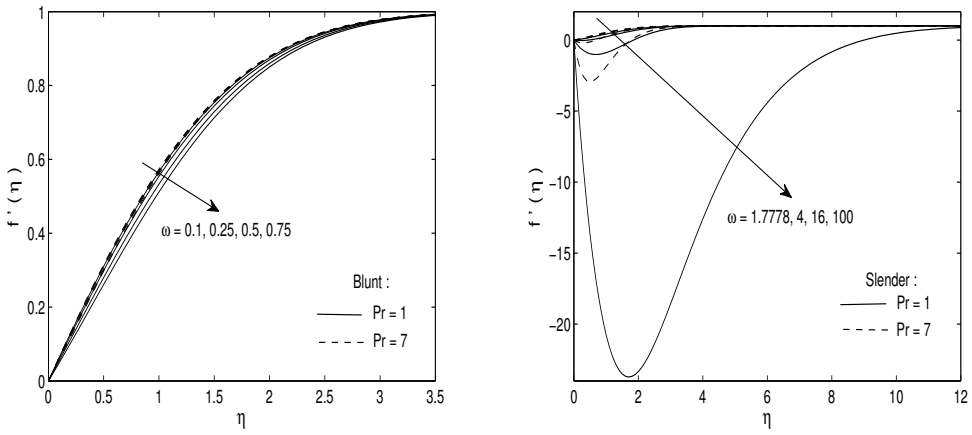

(a) (b)

Figure 6: The velocity profiles at $x = 0$ (forward stagnation point) for some values of ω and Pr when $t = 0.15$ and $\alpha = -3$ in (a)blunt orientation ($\omega = 0.5$) and (b)slender orientation ($\omega = 4$)

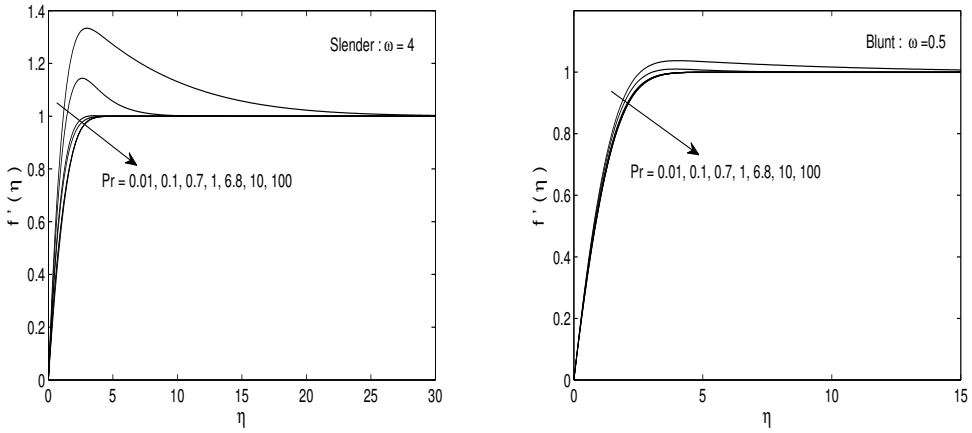

(a) (b)

Figure 7: The velocity profiles at $x = 0$ (forward stagnation point) for some values of Pr when $t = 0.15$ and $\alpha = 1$ in (a)slender orientation ($\omega = 4$) and (b)blunt orientation ($\omega = 0.5$)

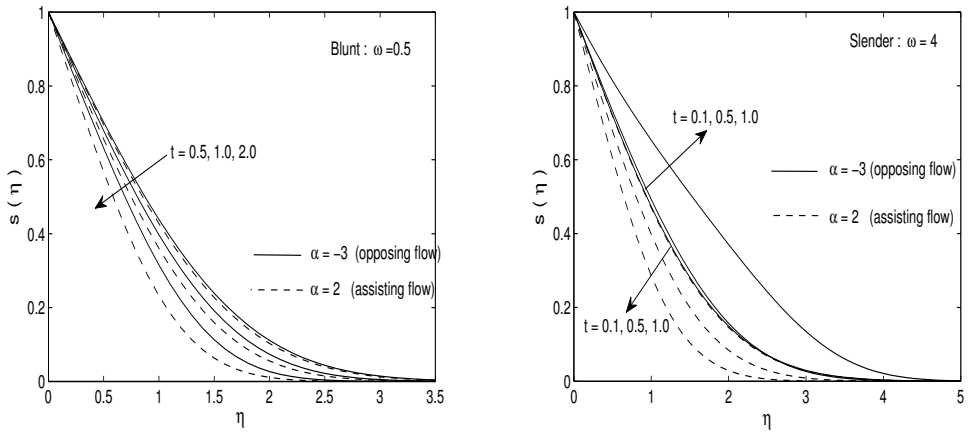

(a) (b)

Figure 8: The temperature profiles at $x = 0$ (forward stagnation point) for some values of α and t when Pr=1 in (a)blunt orientation ($\omega = 0.5$) and (b)slender orientation ($\omega = 4$)

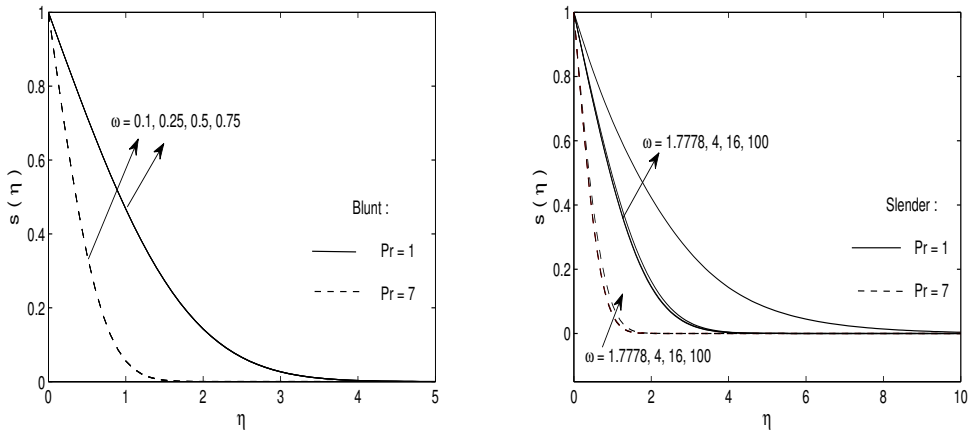

(a) (b)

Figure 9: The temperature profiles at $x = 0$ (forward stagnation point) for some values of ω and Pr when t=0.15 and $\alpha = -3$ in (a)blunt orientation and (b)slender orientation

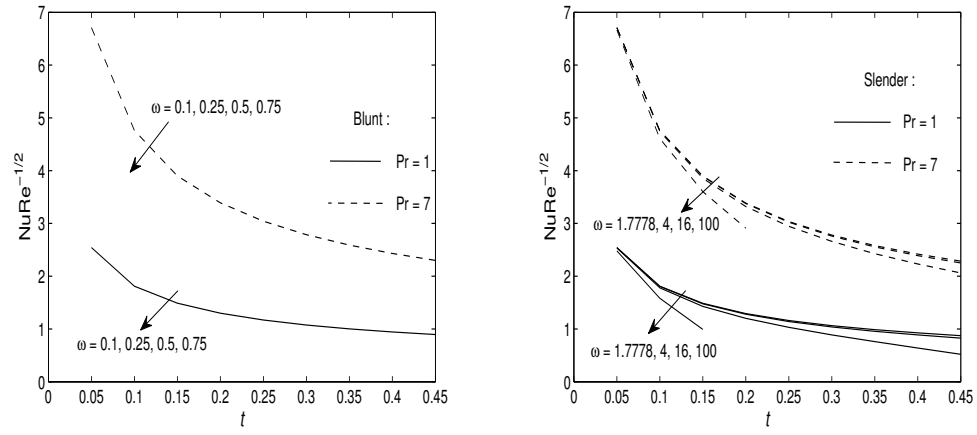

(a) (b)

Figure 10: Variation of the Nusselt number with t at $x = 0$ (forward stagnation point) for various value of ω and Pr when $\alpha = -3$ for (a)blunt orientation and (b)slender orientation

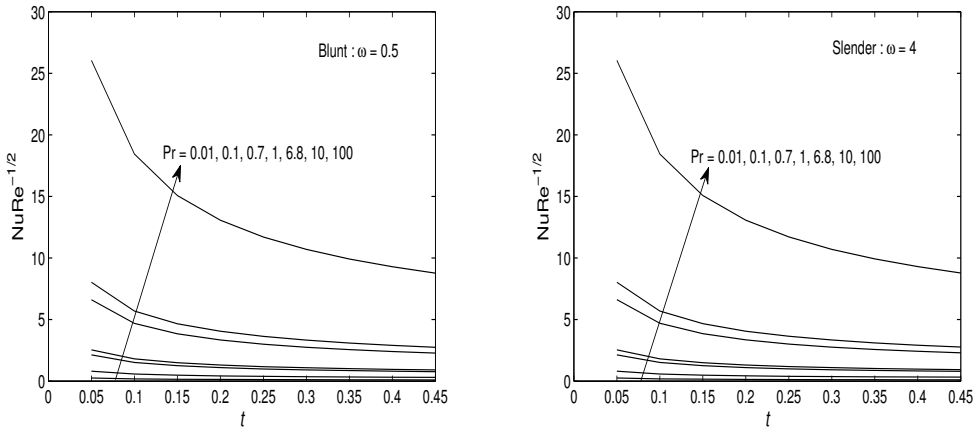

(a) (b)

Figure 11: Variation of the Nusselt number with t at $x = 0$ (forward stagnation point) for various value of Pr when $\alpha = 1$ for (a)blunt orientation and (b)slender orientation

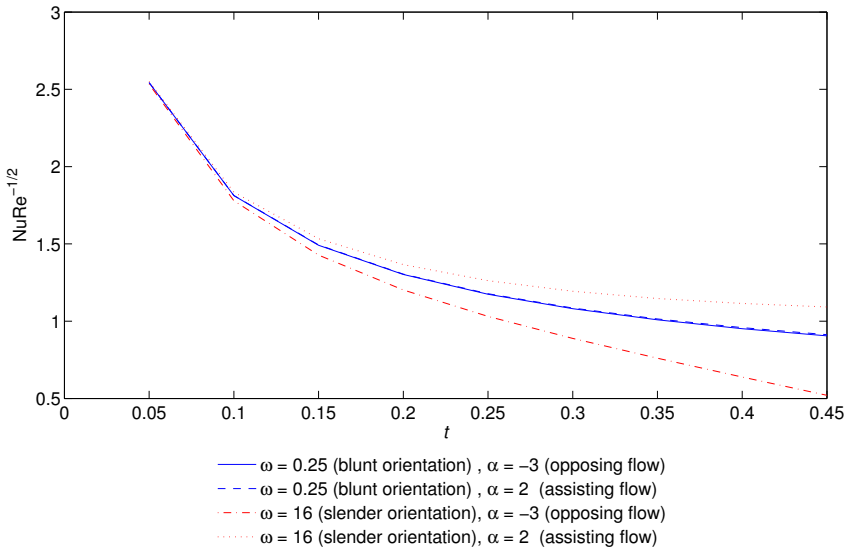

Figure 12: Variation of Nusselt number with t near forward stagnation point for some value of ω and α when Pr=1

References

[1] McCroskey, W. J. Some Current Research in Unsteady Fluids Dynamics. *Journal of Fluids Engineering*. 1977. 99(1): 8-39.

[2] Ingham, D. B. and Merkin, J. H. Unsteady Mixed Convection from an Isothermal Circular Cylinder. *Journal of Acta Mechanica*. 1981. 38: 55-69.

[3] Ali, A., Amin, N., and Pop,I. (2010). Unsteady Mixed Convection Boundary Layer from a Circular Cylinder in a Micropolar Fluid. *International Journal of Chemical Engineering*. 1-10.

[4] Lok, Y. Y. Mathematical Modeling of a Micropolar Fluid Boundary Layer Near a Stagnation Point. Universiti Teknologi Malaysia, Skudai: Ph. D. Thesis. 2008.

[5] Merkin, J. H. Free Convection Boundary Layers on Cylinders of Elliptic Cross Section. *Journal of Heat Transfer*. 1977. 99: 453-457.

[6] D'Alessio, S. J. D. and Dennis, S.C.R. Steady Laminar Forced Convection from an Elliptic Cylinder. *Journal of Engineering Mathematics*. 1995. 29: 181-193.

[7] Chadna, A. *Flow Past an Elliptic Cylinder*. University of Windsor, Ontario, Canada. 1995.

[8] Choi, J. H. and Lee, S. J. Ground Effect of Flow around an Elliptic Cylinder in a Turbulent Boundary Layer. *Journal of Fluids and Structures*. 2000. 14: 697-709.

[9] Khan, W. A., Culham, J. R. and Yovanovich, M. M. Fluid Flow and Heat Transfer from Elliptical Cylinders: Analytical Approach. *Journal of Thermophysics and Heat Transfer*. 2005. 19(2): 178-185. American Institute of Aeronautics and Astronautics Inc.

[10] El-Bashir, T. B. A. Creeping Flow Past an Elliptical Cylinder in the Presence of a Vortex. In *Proceeding of the 5th IASME/WSEAS International Conference on Fluid Mechanics and Aerodynamics*. August 25-27, 2007. Athens, Greece. 36-42.

[11] Mushtaq, M., Nazir, S., Shah, N.A., and Muhammad, G. Calculation of Potential Flow around an Elliptic Cylinder using Boundary Element Method. *Journal of Mathematical Sciences and Mathematics Education*. 2010. 5(1): 37-51.

[12] D'Alessio, S. J. D., and Young, P. J. S. Steady Flow Past an Elliptic Cylinder Inclined to the Stream. *Journal of Engineering Mathematics*. 2003. 47: 101-120.

[13] Bhattacharyya, S. and Pop, I. Free Convection from Cylinders of Elliptic Cross-Section in Micropolar Fluids. *International Journal of Engineering Science*. 1996. 34(11): 1301-1310.

[14] Cheng, C-Y. Free Convection Heat and Mass Transfer From a Horizontal Cylinder of Elliptic Cross Section in Micropolar Fluids. *International Communications in Heat and Mass Transfer*. 2006. 33: 311-318. Elsevier Limited.

[15] Cheng, C-Y. A boundary layer analysis of heat transfer by free convection from permeable horizontal cylinders of elliptic cross-section in porous media using a thermal non-equilibrium model. *International Communications in Heat and Mass Transfer*. 2007. 34: 613-622.

[16] Bharti, R. P., Sivakumar, P. and Chhabra, R. P. Forced Convection Heat Transfer From an Elliptical Cylinder to Power-Law Fluids. *International Journal of Heat and Mass Transfer*. 2008. 51: 1838-1853.

[17] Rao, P. K., Sahu, A. K., and Chhabra, R. P. Flow of Newtonian and Power-Law Fluids past an Elliptical Cylinder: a Numerical Study. *Industrial and Engineering Chemistry Research*. 2010. 49: 6649-6661.

[18] Facas, G. N. Natural Convection from a Buried Elliptic Heat Source. *International Journal of Heat and Fluid Flow*. 1995. 16: 519-526.

[19] Hossain, M. A., Alim, M. A. and Rees, D. A. S. Effect of Thermal Radiation on Natural Convection over Cylinders of Elliptic Cross Section. *Acta Mechanica*. 1998. 129: 177-186.

[20] Cheng, C-Y. Natural Convection Heat Transfer from a Horizontal Isothermal Elliptical Cylinder with Internal Heat Generation. *International Communications in Heat and Mass Transfer*. 2009: 36. 346-350.

[21] Ahmad, S., Arifin, N. M., Nazar, R. and Pop, I. Free Convection Boundary Layer Flow over Cylinders of Elliptic Cross Section with Constant Surface Heat Flux. *European Journal of Scientific Research*. 2008. 23: 613-625.

[22] D'Alessio, S. J. D, Finlay, L. A. and Pascal, J. P. Free Convection from Elliptic Cylinders at Small Grashof Numbers. *International Journal of Heat and Mass Transfer*. 2008. 51: 1379-1392.

[23] D'Alessio, S. J. D., and Perera, R. N. Unsteady Free Convection from Elliptic Cylinders at Large Grashof Numbers. *International Journal of Heat and Mass Transfer*. 2009. 52: 5940-5953.

[24] D'Alessio, S. J. D. Steady and Unsteady Forced Convection past an Inclined Elliptic Cylinder. *Acta Mechanica*. 1997. 123: 99-115.

[25] Ali,A. *Unsteady Micropolar Boundary Layer Flow and Convective Heat Transfer*. Universiti Teknologi Malaysia: Ph. D Thesis. 2010.

[26] Ali, A., Amin, N., and Pop, I. The Unsteady Boundary Layer Past a Circular Cylinder in a Micropolar Fluid. *International Journal of Numerical Methods for Heat and Fluids Flow*. 2007. 17(7): 692-714.